
UNIVERSITY
OF WOLLONGONG
AUSTRALIA

University of Wollongong
Research Online

Faculty of Science, Medicine and Health - Papers: Part B

Faculty of Science, Medicine and Health

2018

Raman spectroscopy of lipid micro-residues on Middle Palaeolithic stone tools from Denisova Cave, Siberia

Luc Bordes
University of Wollongong, lfb437@uowmail.edu.au

Richard Fullagar
University of Wollongong, fullagar@uow.edu.au

Linda C. Prinsloo
University of Wollongong, lprinslo@uow.edu.au

Elspeth Hayes
University of Wollongong, ehh998@uowmail.edu.au

Maxim Kozlikin
Altai State University

See next page for additional authors

Publication Details

Bordes, L., Fullagar, R., Prinsloo, L. C., Hayes, E., Kozlikin, M. B., Shunkov, M. V., Uliyanov, V. A., Derevianko, A. P. & Roberts, R. G. (2018). Raman spectroscopy of lipid micro-residues on Middle Palaeolithic stone tools from Denisova Cave, Siberia. Journal of Archaeological Science, 95 52-63.

Research Online is the open access institutional repository for the University of Wollongong. For further information contact the UOW Library: research-pubs@uow.edu.au

Raman spectroscopy of lipid micro-residues on Middle Palaeolithic stone tools from Denisova Cave, Siberia

Abstract

Raman spectroscopy is a powerful method for detecting micro-residues on stone tools. To further develop techniques for determining stone tool function, we devised a methodology using Raman microscopy to analyse in situ micro-residues before conventional usewear study. We analysed 18 stone artefacts collected in situ from Denisova Cave in Siberia, where excellent organic residue preservation is expected. We report here details of saturated and unsaturated fatty acids identified on eight stone tools from the Middle Palaeolithic levels. The spatial distribution of smeared fatty acids shows strong correlation with spatial distributions of usewear (particularly use-polish, but also striations, edge rounding and scarring) on each tool, demonstrating that these micro-residues are likely associated with prehistoric tool contact with animal tissue. We compared Raman spectra and the types, abundance and distribution of micro-residues on the Denisova Cave artefacts with those on modern experimental stone tools (with known function). The results provide further support for Middle Palaeolithic processing of animal tissue and probable skin scraping at Denisova Cave.

Publication Details

Bordes, L., Fullagar, R., Prinsloo, L. C., Hayes, E., Kozlikin, M. B., Shunkov, M. V., Uliyanov, V. A., Derevianko, A. P. & Roberts, R. G. (2018). Raman spectroscopy of lipid micro-residues on Middle Palaeolithic stone tools from Denisova Cave, Siberia. Journal of Archaeological Science, 95 52-63.

Authors

Luc Bordes, Richard Fullagar, Linda C. Prinsloo, Elspeth Hayes, Maxim Kozlikin, Michael Shunkov, Vladimir A. Uliyanov, Anatoly Derevianko, and Richard G. Roberts

This journal article is available at Research Online: https://ro.uow.edu.au/smhpapers1/26

*Manuscript
Click here to view linked References

Raman spectroscopy of lipid micro-residues on Middle Palaeolithic stone tools from Denisova Cave, Siberia

Luc Bordes[a], Richard Fullagar[a], Linda C. Prinsloo[a], Elspeth Hayes[a], Maxim B. Kozlikin[b,c], Michael V. Shunkov[b,d], Anatoly P. Derevianko[b,c], Richard G. Roberts[a,e,*]

[a] Centre for Archaeological Science, School of Earth and Environmental Sciences, University of Wollongong, Wollongong, New South Wales 2522, Australia

[b] Institute of Archaeology and Ethnography, Russian Academy of Sciences, Siberian Branch, Novosibirsk, RU-630090, Russia

[c] Altai State University, Barnaul, RU-656049, Russia

[d] Novosibirsk National Research State University, Novosibirsk, RU-630090, Russia

[e] Australian Research Council (ARC) Centre of Excellence for Australian Biodiversity and Heritage, University of Wollongong, Wollongong, New South Wales 2522, Australia

* Corresponding author: rgrob@uow.edu.au

ABSTRACT

Raman spectroscopy is a powerful method for detecting micro-residues on stone tools. To further develop techniques for determining stone tool function, we devised a methodology using Raman microscopy to analyse in situ micro-residues before conventional usewear study. We analysed 18 stone artefacts collected in situ from Denisova Cave in Siberia, where excellent organic residue preservation is expected. We report here details of saturated and unsaturated fatty acids identified on eight stone tools from the Middle Palaeolithic levels. The spatial distribution of smeared fatty acids shows strong correlation with spatial distributions of usewear (particularly use-polish, but also striations, edge rounding and scarring) on each tool, demonstrating that these micro-residues are likely associated with prehistoric tool contact with animal tissue. We compared Raman spectra and the types, abundance and distribution of micro-residues on the Denisova Cave artefacts with those on modern experimental stone tools (with known function). The results provide further support for Middle Palaeolithic processing of animal tissue and probable skin scraping at Denisova Cave.

Keywords: fatty acids, stone artefacts, usewear, microwear, tool function, animal skin processing

1. Introduction

As underscored by previous analysts, the visual characterisation of micro-residues using optical microscopes is challenging when the residues lack distinct shapes or structures (Langejans, 2012; Monnier et al., 2012, 2017a,b; Wadley et al., 2007). In these conditions, micro-residues resulting from stone tool use also pose challenges because they are more difficult to distinguish from modern contaminants, mineral background or from the effects of post-depositional processes (Langejans, 2010).

Spectroscopic analyses have been applied previously to characterise visible traces of glue and adhesive compounds, after macroscopic or low-magnification observations (e.g., Cârciumaru et al., 2012; Vahur et al., 2011). Similarly, microscopic usewear studies have been complemented by subsequent application of spectroscopic techniques (e.g., infrared and Raman spectroscopy) to residues potentially linked with utilised tool edges (e.g., Cesaro et al., 2012; Hogberg et al., 2009). Other studies have applied Raman or infrared spectroscopy at a later stage of functional analysis, to confirm origins of organic residues that were previously identified as distinct structures by optical microscopy (Monnier et al., 2013, 2017a,b). To confirm that micro-residues are related to prehistoric tool use and not the outcome of another agency (such as contamination from handling or sediments), it is important to assess multiple lines of evidence (e.g., Lombard et al., 2009), including micro-residue abundance and meaningful distributions (Rots et al., 2016). For example, micro-residues that are distributed widely on artefact surfaces may potentially be a consequence of contact with sediment (or various taphonomic processes) rather than tool use, which typically constrains impacted residues close to used tool edges.

Previous studies have shown that it is usually appropriate to record and document residues before undertaking detailed usewear analysis, which often requires cleaning of tools to observe wear on tool surfaces (Keeley, 1980). In situ, non-destructive study of residues should be undertaken before residues are removed for chemical and other testing. A common first step in study of tool residues is optical microscopy to identify tools and residues that may then be subjected to further testing. In this study, prehistoric stone tools were not first selected on the basis of optical microscopy or any macro-residues. Our study aimed to evaluate Raman microscopy (Raman spectroscopy with optical microscope capabilities) as a non-destructive method of in situ residue analysis independent of microwear analysis—'independent' in the sense that Raman microscopy is undertaken first and, thus, tools are not subject to residue alteration, removal or contamination by prior analysis. This independence, however, poses particular challenges when initial functional interpretations are not available to limit the areas of observation, or to suggest potential utilised materials, modes of use and utilised edges. First, the analyst is not assisted by prior optical microscopy cues or related techniques (e.g., chemical staining) to infer the nature or origin of residues. Second, to be viable and effective, the analytical technique must be rapid enough to efficiently scan and probe hundreds of micro-residues on stone surfaces and edges. The analytical technique should have the capacity for rapid chemical analysis (within a few seconds) to provide adequate sample coverage of tools, commonly with surface areas on the order of

~10–50 cm^2. Relocating the same tool residue under different instruments would be very time consuming, so the use of a single instrument for optical microscopy and chemical analysis is highly advantageous.

We argue that Raman microscopy is a viable 'independent' methodology for initially locating and analysing in situ micro-residues on prehistoric stone artefacts. Recently, we confirmed that Raman microscopy has particular advantages for the early examination of stone artefacts after initial screening with conventional usewear/residue observations (Bordes et al., 2017). Bordes et al. (2017) showed that Raman microscopy of unwashed artefacts can identify archaeologically significant organic traces with minimal artefact handling (to reduce the chances of contamination) and with minimal cleaning (<10 s ultrasonication in water); the latter removed loosely adhering sediment without dislodging residues related to tool use.

To evaluate Raman microscopy as the first step of in situ residue observation (i.e., prior to conventional usewear/residue observations), we selected in situ artefacts that had been carefully collected from the Denisova Cave deposits for residue analysis. This site was chosen for study because it has excellent conditions for organic preservation over many tens of millennia, as shown by the survival of ancient DNA and collagen peptides in the skeletal remains of archaic hominins (Brown et al., 2016; Meyer et al., 2012; Prüfer et al., 2014) and in the cave sediments (Slon et al., 2017). To assist in interpreting our results, modern experimental tools were also analysed with Raman microscopy.

2. Denisova Cave and artefact selection

Denisova Cave is located on the northwest slopes of the Altai Mountains in southern Siberia. It provides an excellent geographic environment for evaluating our methodology, given the cold, relatively stable conditions in the buried cave deposits and an archaeological record that extends as far back as the late Middle Pleistocene (Derevianko et al., 2003, 2005; Slon et al., 2017). Archaic hominins (Denisovans and Neanderthals) and modern humans have occupied the cave at various times.

The 18 stone tools reported here were collected in 2014 from Layers 15 to 11.4 in the East Chamber of the cave. These layers have yielded Middle Palaeolithic lithic artefacts, as well as the remains of Denisovans and Neanderthals (Brown et al., 2016; Meyer et al., 2012; Prüfer et al., 2014; Slon et al. 2017). The stones were removed, with minimal handling, from the section walls and stored in plastic bags, which were left open to air dry before being sealed for transport to the University of Wollongong for analysis. Sediment samples were collected for each stone, and included: (1) sediment in contact with the stone surface ('inner sediment sample') and (2) sediment up to 3 cm distant from the stone surface ('outer sediment sample').

Our objective was to assess how these stone tools were used and what plants and animals they were used to process. Preliminary studies of Pleistocene mammal remains in the East Chamber (Vasiliev et al., 2008, 2010, 2013, 2017) indicate the dominance of forest taxa (especially roe deer and Siberian red deer) in Layers 15

and 14, followed by a progressive increase in the proportion of steppe taxa in the overlying Late Pleistocene deposits. These environmental changes may have influenced hominin subsistence strategies and, hence, tool function.

3. Methods

3.1. Raman and optical microscopy

Raman spectra were recorded with a WITec Alpha 300R confocal Raman microscope (WITec. Instrument Corp., Germany) equipped with two UHTS300 spectrometers and two CCD detectors: (1) a visible DV401 detector for use with 532 nm excitation; and (2) a DV401 detector for 785 nm excitation. The excitation sources were two diode lasers operated at 532 nm and 785 nm wavelengths with 38 mW and 120 mW maximum power output, respectively. Zeiss microscope objectives (20× and 50× magnifications) were used, achieving a sub-micron resolution. The samples were placed on a piezo-driven, feedback-controlled scanning stage.

To avoid contamination, artefacts were handled with nitrile gloves (latex, powder- and protein-free), and placed on a support fashioned by Blu-Tack® (a synthetic rubber compound) to accommodate its shape. This enabled the positioning of each sample under the Raman microscope with the incident light (laser) normal (i.e., perpendicular) to the point of analysis. The support was covered with a piece of nitrile glove to prevent contamination from the Blu-Tack®. Samples were stored in clean bags and boxes before and after analysis.

Optical microscopes included an Olympus stereozoom SZ61 with external fibre optic light source, and an Olympus BX51 metallographic microscope with vertical incident illumination and 5×, 10×, 20× and 50× objectives.

3.2. Analytical steps

Artefacts were analysed in six steps (analyst(s) indicated below in parentheses), with extra Step 1a for the first five artefacts examined (details in Table 1):

(1) Catalogue unwashed artefacts (E.H. and R.F.).
  (1a) Optical microscopy of microwear and residues on DC2, DC12, DC22, DC42 and DC52 (E.H. and R.F.). Following study of these initial five artefacts, Step 1a was eliminated to reduce the total analysis time, render the Raman microscopy independent of prior optical study, and reduce the chance of modern contamination.
(2) Raman microscopy of residues on artefacts prior to cleaning (L.B.).
(3) Ultrasonication of artefacts (L.B.).
(4) Raman microscopy of residues and sediments (L.B.).
(5) Optical microscopy and mapping of use-polish (L.B.).
(6) Optical microscopy of usewear and residues (R.F. and E.H.).

3.3 Experimental tools

Experimental stone-tool residues of more recent age were analysed to aid in the

interpretation of residues on the Denisova Cave artefacts. The experimental tool residues included two sets, each of a different age: tools used ~30 years earlier (Set 1; Fullagar 1986) and tools used up to ~9 months earlier (Set 2). See Table 2 for details.

Set 1 included residues on four tools used to process animal tissue: (1) hornfels X290, used for scraping fresh skin (possum, *Trichosurus vulpecula*) for 5 min; (2) flint X284, used for sawing dry bone (cow, *Bos taurus*) for 20 min; (3) flint X288, used for cutting fresh meat (cow) for 20 min; and (4) flint X309, used for sawing fresh bone (cow) for 45 min. Residues on these four experimental tools were investigated specifically to study lipid preservation and characterise their Raman spectra after ~30 years of storage in stable conditions (details in Table 2).

Set 2 included residues on nine tools made of stones of similar rock types to those recovered from the Middle Palaeolithic levels at Denisova Cave (siltstone, quartzite, and fine-grained volcanic rock) and collected in the vicinity of the site. Tools D1–3 were used to process deer bone and skin (removed from the carcass three months after death in Australia) and were analysed immediately or shortly after use. These tools were used for: extracting marrow/scraping bone (D1); sawing bone (D2); and scraping skin (D3). Five of the six remaining tools were used to collect and process plant materials found in the vicinity of Denisova Cave and documented in the palynological records (Bolikhovskaya and Shunkov, 2014; Derevianko et al., 2003): cutting fern (D4, analysed after two weeks); cutting and scraping rowan wood (D5, analysed after two weeks); cutting and scraping Siberian pine (D8, analysed after one month); cutting nettle (D9, analysed after nine months); and cutting birch wood (D10, analysed after one month). The sixth tool (D11) was used to cut and process tussock grass collected in Australia and analysed after one day.

None of the experimental tools from Set 1 or Set 2 were washed or cleaned prior to analysis. Residues sometimes obscured part of the stone surface, but it was feasible to directly investigate residues and their association with edge-rounding and polished zones under the Raman microscope, and to record spectra and images for comparison with the optical microscopy data.

4. Results

The Denisova Cave artefacts analysed with Raman microscopy include seven flakes, seven retouched flakes and four other flaked pieces (Table 3). Lipid micro-residues were detected on eight out of the 18 artefacts analysed. Table S1 lists the Raman bands used for residue and mineral identification.

Raman microscopy of artefacts before ultrasonication (Step 2) was limited because a thick coating of sediment hampered observation of organic residues and contributed to a high fluorescence background. Micro-residues detected at Step 2 consisted almost entirely of modern contaminants (e.g., plant fibres and modern dyed fibres on DC2 and DC12) and a few apatite micro-residues in the sediment attached to DC2. It was not possible to detect any residues on DC4 or DC13, due to the thickness of the

sediment layer attached. After 10 s ultrasonication (Step 3), distinctive distributions of micro-residues could readily be observed. Accordingly, the data presented below were collected in step 4 and step 5.

4.1 Artefacts DC2 and DC12

All residues were optically distinguished using the 50× objective, and, to avoid confusion with pseudomorph mineral grains, systematic Raman analysis was performed to confirm their chemical nature. Although the emphasis of this paper is on lipid residues, Table 4 presents a summary of all the micro-residues detected on artefacts DC2 and DC12 and their relative occurrence. Table 4 also summarises the minerals and micro-residues in the outer and inner sediment samples and in the washed sediment obtained during ultrasonication; the results for the inner and outer sediments are indistinguishable for each artefact, so they have been grouped together.

Lipid micro-residues were observed on both artefacts as white solid features with a grainy texture (Fig. 1A–E). These discrete micro-residues, with clear shapes and boundaries, are labelled as individual micro-residues with similar Raman spectra (e.g., Fig. 1F). The spectra are typical of saturated fatty acids (SFA), characterised by very strong CH_2 and CH_3 stretching vibrations (2800–2950 cm^{-1}), bending CH_2/CH_3 vibrational bands at 1466 and 1443 cm^{-1}, a CH_2 twisting mode at 1299 cm^{-1}, and C-C stretching at 1132, 1104 and 1066 cm^{-1} (Czamara et al., 2015; De Gelder et al., 2007). Additionally, three low-intensity broad bands at 1571, 1603 and 1657 cm^{-1} occur in the spectra, indicating that other minor compounds may be present. The spectrum closely resembles that of palmitic and stearic acid and is similar to fatty acid spectra recorded on stone tools from Liang Bua (Bordes et al., 2017). Although it is possible to distinguish between saturated fatty acids based on the position and relative intensity of various bands, it is not possible for most of the spectra recorded here as the residues are mixtures and, in many instances, spectrum quality is not optimum. However, it is worth mentioning that all SFA spectra recorded on DC26 and DC27 are markedly different from the spectra recorded for SFA on the other artefacts (Fig. S1). The main difference is the lower intensity ratio of the CH_2 twisting mode (1300 cm^{-1}) and C-C stretching modes (1134, 1104 and 1067 cm^{-1}) compared to the main bending CH_2/CH_3 vibrational bands at 1464 and 1446 cm^{-1}. This variation in the Raman signal may reflect differences in the ratio between palmitic and stearic acid.

Another residue type was also observed as a thin film smeared on the surfaces of DC2 and DC12. These films were only visible microscopically, even for the apparently thicker smeared zones (Fig. 2) and they can be sometimes observed overlying and fitting polish striations (Fig. 2A,C,D) on DC2 and DC12, and on DC26 and DC27 (Fig. S1A–D). The Raman spectra were identical to those obtained for individual SFA micro-residues, and spectral imaging confirmed their spatial distribution on the rock surface as thin discontinuous films (Fig. 3). To distinguish them from individual SFA micro-residues, we refer to them as ‘smeared SFA micro-residues’. The intensity of the Raman signal decreased rapidly when the microscope

objective was moved slightly out of focus in either direction, whereas the mineral background signal increased with downward focusing, indicating that the films are only a few microns deep. Most surfaces covered with smeared SFA correspond to polished areas and the smears are not homogeneous in thickness, but infill the irregularities and cracks in the polished surface. Figure 4 shows the distribution of micro-residues on artefacts DC2 and DC12 in relation to areas and edges with polish.

4.2 Artefacts DC4 and DC13

Similar to artefacts DC2 and DC12, individual (Fig. 5A,B) and smeared lipid micro-residues (Fig. 5C) were identified on artefacts DC4 and DC13 (Table 4), but some major differences were observed. Individual lipid micro-residues were found in far greater numbers on DC4 and DC13 (Fig. 4) and have a different appearance, namely a more delicate structure than the solid white micro-residues found on DC2 and DC12. In a similar way as DC2 and DC12, smeared micro residues can be sometimes observed overlying and fitting polish striations (Fig. 5C,D). Moreover, the micro-residues on DC4 and DC13 can be found clustered and more often concentrated around smeared residues (Fig. 5D). The corresponding Raman spectra have additional peaks at 1656 and 3010 cm^{-1} (C=C stretch cis isomer and =C-H stretching, respectively) and a shoulder centred at 1260–1270 cm^{-1} (=C-H deformation) (Fig. 5E and 6A,B), which can be attributed to unsaturated fatty acids (Czamara et al., 2015; De Gelder et al., 2007). The presence of another C=C stretch band centred at 1679 cm^{-1} suggests the presence of a trans isomer (Czamara et al., 2015) and a band at 1610 cm^{-1} (Fig. 6A) might be attributable to a conjugated cis isomer mode with multiple C=C-C=C modes (Melchiorre et al., 2015). Presence of these unsaturated spectral markers indicates that individual and smeared lipid micro-residues on DC4 and DC13 are a mixture of saturated and unsaturated fatty acids. We refer to these micro-residues as ‘SFA/UFA’ to distinguish them from micro-residues of pure SFA composition found on DC2 and DC12.

4.3 Experimental stone tools

The analysis of residues on experimental tools used to process known materials provides a basis for interpreting the mode of deposition of lipid micro-residues on archaeological artefacts and detection range of Raman spectroscopy. Table 2 summarises the micro-residues detected on the experimental tools, including information on their relative abundance, worked material, tasks performed with the tool, and time elapsed before analysis.

The material processed using the tools can be divided into animal and plant groups. The experimental tools from Set 1 were used to process animal tissue ~30 years ago and the residues identified include individual and smeared saturated fatty acids, bone and collagen. Set 2 experimental tools D1, D2 and D3 were used to process bone and skin; the resulting residues are analogous to those found on archaeological tools DC4 and DC13, with some residues consisting of SFA/UFA mixtures (e.g., D3 in Fig. S2). Hence, for the experimental tools used ~30 years ago and since stored at ambient temperatures in Australia, the fatty acids have degraded to their saturated

counterparts.

The most common residues identified on the Set 2 tools used to process fresh plant material (fern, rowan, Siberian pine and birch bark) include plant fibres, wood fibres and, in a few instances, carotenoid pigments (on D4, used to cut fern). Interestingly, for the tool used to cut nettle (D9), a plant rich in natural oils, the Raman spectra are comparable to those documented for tools used to process deer fat and for Denisova Cave artefact DC4 and experimental tool D3 (Fig. 7). Consequently, the spectra of saturated and unsaturated lipids obtained for these experimental tools are not diagnostic of the material processed, but, nevertheless, the relative abundance of micro-residues can provide complementary information. Indeed, Table 2 shows the relative amounts of residue types for the experimental tools used to process different materials, and their association with other tool residues. Bone and collagen residues were most common on artefacts used to saw or cut bone, while collagen fibres and smeared proteins were more common on tools used to cut meat. Scraping animal skin resulted in numerous fatty acid residues, some occurring as discrete residues with a specific shape (Fig. S2) and others spread over a large area (Fig. S3), often covering continuously parts of polished tool edges. The relative abundance of lipid micro-residues varies widely among the experimental tools used for processing different plants (Table 2) and smeared lipids were also observed, but not in such large numbers as lignin and cellulose plant fibres.

5. Discussion

As lipids are expected to be relatively well preserved compared to carbohydrates, proteins and nucleotides, they are excellent candidates for use in archaeological investigations (Evershed, 1993; Luong et al., 2017). Lipids occur as triglycerides (esters of glycerol and three fatty acids) in both plants and animals, but over time break down to glycerol and free fatty acids. Under ideal preservation conditions, saturated and unsaturated fatty acids have been shown to survive well in mammal remains found in permafrost, as identified by gas chromatography-mass spectrometry (GC-MS) (e.g., Guil-Guerrero et al., 2014). GC-MS has also revealed the occurrence of lipids on archaeological artefacts, including a 9000-year-old pottery sherd from the Jomon site in Japan (Lucquin et al., 2016) and a collection of burnt rocks from a Late Archaic Period site in south Texas (Buonasera, 2005).

We consider the lipid micro-residues documented on the Denisova Cave artefacts to be use-related, because: (1) they are distributed along the working edges in correlation with polished zones; and (2) they are absent from the sediment samples and on unused portions of the stones. SFA micro-residues were found on four artefacts (DC2, DC12, DC26 and DC27), corresponding to two different Raman spectra (see distinction between SFA and SFA' in Table 3). SFA/UFA mixtures were found on four other artefacts (DC4, DC11, DC13 and DC39). Figure S4 shows the distribution of micro-residues on artefacts DC11, DC26, DC27 and DC39 in relation to areas and edges with polish. We regard the micro-residues on DC4, DC11, DC13 and DC39 as the best preserved, for two reasons: (1) saturated fatty acids have a higher melting point than unsaturated fatty acids (for fatty acids of similar carbon-

chain length) and are solids at ambient temperature, whereas unsaturated fatty acids are liquid (oil); and (2) unsaturated fatty acid micro-residues degrade over time into saturated fatty acids (Regert et al., 1998).

Our experiments have indicated that spectral signatures of lipid micro-residues alone may be insufficient to identify the worked material, as the spectra cannot at this stage distinguish definitively between plant and animal residues (Table 2 and Fig. 7). For the Denisova Cave artefacts, we also have to incorporate other observations to infer tool use. We suggest that micro-residues of plant or animal origin may be distinguished on the basis of: (1) how they appear on each artefact surface (i.e., as individual or smeared micro-residues); and (2) their relative abundance on the tool surface. Analysis of our experimental tools indicates that lipid micro-residues occur in relatively high abundance on tools used to work animal materials (Table 3). Tissue layers under skin and fresh bone marrow are rich in fat, leading to a larger quantity of smeared and individual lipid micro-residues along the utilised portions of the tools.

Fatty acid micro-residues can occur on tools used to process both plant and animal tissue, but fatty acids occur less frequently than other plant tissues on tools used to process plants. Previous studies in archaeological contexts have indicated that lignin and plant polymers are less susceptible to structural modification and degradation than lipids (Evershed 1993), so plant residues are expected to be more abundant than lipids on archaeological tools used to process plant materials. The presence of fatty acid micro-residues on several artefacts (DC2, DC4, DC12, DC13, DC26 and DC27) on which plant tissues are mostly absent might indicate, therefore, that the fatty acids derive mainly from processing of animal tissues, rather than plants, thereby supporting our interpretation that these tools were used to work animal materials. Plant tissues occur in very low frequencies on DC1 and DC2 as isolated plant fibres and as starch grains on DC4 (n = 1) and DC12 (n = 2). Given these rare occurrences, we cannot confidently link them with the main use of these artefacts; they may instead be incidental or derive from modern contamination.

Small particles of apatite are present on the Denisova Cave artefacts, but these cannot be clearly related to their use. Apatite was common on all 18 artefacts and may be a degradation product from bone apatite or precipitated from the sediment. Solid bone fragments were not optically identified, however, and the distribution of apatite crystals displayed no apparent patterning and was not associated with other wear traces, such as polish. In addition, artefacts recovered from Layer 11.4 had a continuous layer of apatite extending across entire surfaces, indicating that the apatite probably derives from the surrounding sediment. Analysis of the latter confirms this interpretation, with phosphate particles being the most common mineral grains identified in all sediment samples.

The presence of individual and smeared SFA and UFA micro-residues, with the absence of bone and plant micro-residues, indicates that the Denisova Cave artefacts were most likely used to work animal skins. This interpretation is in agreement with the subsequent studies of usewear in Step 6 (Table 3). Raman

microscopy and conventional usewear and residue analysis are complementary approaches, each offering the potential to provide unique information about tool function. Raman microscopy can provide greater detail about the worked materials and is especially useful when inferences from conventional microscopy are ambiguous (e.g., DC26, Table 2).

6. Conclusions

Determining the origins of micro-residues and how these relate to prehistoric tool use is necessary for robust functional analyses. For a residue to be considered related to tool use, multiple organic micro-residues need to have a demonstrated relationship with distributions of polish and other usewear. Our study shows that the high spatial resolution of Raman microscopy makes it a valuable technique for determining the probable origin of residues on stone tools. Moreover, we have shown that Raman microscopy can be particularly useful when deployed prior to conventional usewear and residue analysis, and can reliably identify individual and smeared micro-residues that may be directly related to tool function. Raman microscopy and conventional usewear and residue studies provide a complementary means of inferring tool function.

We have been able to infer the function of Middle Palaeolithic tools that were probably used to work animal tissues at Denisova Cave. Comparison of the archaeological micro-residues with aged and fresh micro-residues on experimental stone tools supports our hypothesis of animal skin processing as the main function of at least four tools (DC2, DC4, DC12 and DC13) recovered from Layer 11.4 in the East Chamber of Denisova Cave. In this study, we have focussed on linking the spatial distribution of micro-residues as determined with Raman spectroscopy to polish/usewear distribution, and identified three different fatty acid Raman spectral signatures. A more in-depth study of individual spectra, complemented by GC-MS analyses of residues on these and other artefacts, will provide additional information on the nature of the residues. Our study highlights the potential for Raman microscopy to be applied at an early stage of artefact analysis before conventional usewear and residue investigations, and to assist interpretations of resource use and subsistence behaviour by archaic and modern humans.

Acknowledgements

This study was funded by the Australian Research Council through Australian Laureate Fellowship FL130100116 to R.G.R., the Russian Science Foundation through project 14-50-00036 to A.P.D., M.V.S. and M.B.K., and the University of Wollongong through a Postgraduate Award and an International Postgraduate Research Scholarship to L.B. We thank Susan Luong for comments and Vladimir Vaneev for field support.

REFERENCES

Bolikhovskaya, N.S., Shunkov, M.V., 2014. Pleistocene environments of northwestern Altai: vegetation and climate. Archaeol. Ethnol. Anthropol. Eurasia 42/2, 2–17.

Bordes, L., Prinsloo, L.C., Fullagar, R., Sutikna, T., Hayes, E., Jatmiko, Saptomo, E.W., Tocheri, M.W., Roberts, R.G., 2017. Viability of Raman microscopy to identify micro-residues related to tool-use and modern contaminants on prehistoric stone artefacts. J. Raman Spectrosc. 48, 1212–1221.

Brown, S., Higham, T., Slon, V., Pääbo, S., Meyer, M., Douka, K., Brock, F., Comeskey, D., Procopio, N., Shunkov, M., Derevianko, A., Buckley, M., 2016. Identification of a new hominin bone from Denisova Cave, Siberia using collagen fingerprinting and mitochondrial DNA analysis. Sci. Rep. 6, 23559.

Buonasera, T., 2005. Fatty acid analysis of prehistoric burned rocks: a case study from central California. J. Archaeol. Sci. 32, 957–965.

Cârciumaru, M., Ion, R., Nitu, E., Stefanescu, R., 2012. New evidence of adhesive as hafting material on Middle and Upper Palaeolithic artefacts from Gura Cheii-Râsnov Cave (Romania). J. Archaeol. Sci. 39, 1942–1950.

Cesaro, S.N., Lemorini, C., 2012. The function of prehistoric lithic tools: a combined study of use-wear analysis and FTIR microspectroscopy. Spectrochim. Acta A 86, 299–304.

Czamara, K., Majzner, K., Pacia, M.Z., Kochan, K., Kaczor, A., Baranska, M., 2015. Raman spectroscopy of lipids: a review. J. Raman Spectrosc. 46, 4–20.

De Gelder, J., De Gussem, K., Vandenabeele, P., Moens, L., 2007. Reference database of Raman spectra of biological molecules. J. Raman Spectrosc. 38, 1133–1147.

Derevianko, A.P., Shunkov, M.V., Agadjanian, A.K., Baryshnikov, G.F., Malaeva, E.M., Ulianov, V.A., Kulik, N.A., Postnov, A.V., Anoikin, A.A., 2003. Paleoenvironment and Paleolithic Human Occupation of Gorny Altai: Subsistence and Adaptation in the Vicinity of Denisova Cave. Institute of Archaeology and Ethnography, Siberian Branch, Russian Academy of Sciences Press, Novosibirsk.

Derevianko, A.P., Postnov, A.V., Rybin, E.P., Kuzmin, Y.V., Keates, S.G., 2005. The Pleistocene peopling of Siberia: a review of environmental and behavioural aspects. Bull. Indo-Pac. Prehist. Assoc. 3, 57–68.

Evershed, R.P., 1993. Biomolecular archaeology and lipids. World Archaeol. 25, 74–93.

Fullagar, R., 1986. Use-wear and Residues on Stone Tools: Functional Analysis and its Application to Two Southeastern Australian Archaeological Assemblages. PhD thesis, La Trobe University, Australia.

Guil-Guerrero, J.L., Tikhonov, A., Rodriguez-Garcia, I., Protopopov, A., Grigoriev, S., Ramos-Bueno, R.P., 2014. The fat from frozen mammals reveals sources of essential fatty acids suitable for Palaeolithic and Neolithic humans. PLoS One 9, e84480.

Hogberg, A., Puseman, K., Yost, C., 2009. Integration of use-wear with protein residue analysis – a study of tool use and function in the south Scandinavian Early Neolithic. J. Archaeol. Sci. 36, 1725–1737.

Keeley, L.H., 1980. Experimental Determination of Stone Tool Uses: A Microwear Analysis. University of Chicago Press, Chicago.

Langejans, G.H.J., 2010. Remains of the day-preservation of organic micro-residues on stone tools. J. Archaeol. Sci. 37, 971–985.

Langejans, G.H.J., 2012. Micro-residue analysis on Early Stone Age tools from Sterkfontein, South Africa: a methodological enquiry. S. Afr. Archaeol. Bull. 67, 200–213.

Lombard, M., Wadley, L., 2009. The impact of micro-residue studies on South African Middle Stone Age research. In Haslam, M., Robertson, G., Crowther, A., Nugent, S., Kirkwood, L. (Eds), Archaeological Science Under a Microscope: Studies in Residue and Ancient DNA Analysis in Honour of Thomas H. Loy, pp. 11–28. Terra Australis 30, ANU Press, Canberra.

Lucquin, A., Gibbs, K., Uchiyamac, J., Saula, H., Ajimotod, M., Eleya, Y., Radini, A., Heron, C.P., Shoda, S., Nishida, Y., Lundy, J., Jordan, P., Isaksson, S., Craig, O.E., 2016. Ancient lipids document continuity in the use of early hunter–gatherer pottery through 9,000 years of Japanese prehistory. Proc. Natl Acad. Sci. USA 113, 3991–3996.

Luong, S. Hayes, E., Flannery, E., Sutikna, T., Tocheri, M.W., Saptomo, E.W., Jatmiko, Roberts, R.G., 2017. Development and application of a comprehensive analytical workflow for the quantification of non-volatile low molecular weight lipids on archaeological stone tools. Anal. Methods 9, 4349–4362.

Melchiorre, M., Ferreri, C., Tinti, A., Chatgilialoglu, C., Torreggiami, A., 2015. A promising Raman spectroscopy technique for the investigation of trans and cis cholesteryl ester isomers in biological samples. Appl. Spectrosc. 69, 613–622.

Meyer, M., Kircher, M., Gansauge, M.-T., Li, H., Racimo, F., Mallick, S., Schraiber,

J.G., Jay, F., Prüfer, K., de Filippo, C., Sudmant, P.H., Alkan, C., Fu, Q., Do, R., Rohland, N., Tandon, A., Siebauer, M., Green, R.E., Bryc, K., Briggs, A.W., Stenzel, U., Dabney, J., Shendure, J., Kitzman, J., Hammer, M.F., Shunkov, M.V., Derevianko, A.P., Patterson, N., Andrés, A.M., Eichler, E.E., Slatkin, M., Reich, D., Kelso, J., Pääbo, S., 2012. A high-coverage genome sequence from an archaic Denisovan individual. Science 338, 222–226.

Monnier, G.F., Ladwig, J.L., Porter, S.T., 2012. Swept under the rug: the problem of unacknowledged ambiguity in lithic residue identification. J. Archaeol. Sci. 39, 3284–3300.

Monnier, G.F., Hauck, T.C., Feinberg, J.M., Luo, B., Tensorer, J.L., Sakhel, H.A., 2013. A multi-analytical methodology of lithic residue analysis applied to Paleolithic tools from Hummal, Syria. J. Archaeol. Sci. 40, 3722–3739.

Monnier, G., Frahm, E., Luo, B., Missal, K., 2017a. Developing FTIR microspectroscopy for the analysis of animal-tissue residues on stone tools. J. Archaeol. Method Th. https://doi.org/10.1007/s10816-017-9325-3

Monnier, G., Frahm, E., Luo, B., Missal, K., 2017b. Developing FTIR microspectroscopy for analysis of plant residues on stone tools. J. Archaeol. Sci. 78, 158–178.

Prüfer, K., Racimo, F., Patterson, N., Jay, F., Sankararaman, S., Sawyer, S., Heinze, A., Renaud, G., Sudmant, P.H., de Filippo, C., Li, H., Mallick, S., Dannemann, M., Fu, Q., Kircher, M., Kuhlwilm, M., Lachmann, M., Meyer, M., Ongyerth, M., Siebauer, M., Theunert, C., Tandon, A., Moorjani, P., Pickrell, J., Mullikin, J.C., Vohr, S.H., Green, R.E., Hellmann, I., Johnson, P.L.F., Blanche, H., Cann, H., Kitzman, J.O., Shendure, J., Eichler, E.E., Lein, E.S., Bakken, T.E., Golovanova, L.V., Doronichev, V.B., Shunkov, M.V., Derevianko, A.P., Viola, B., Slatkin, M., Reich, D., Kelso, J., Pääbo, S., 2014. The complete genome sequence of a Neanderthal from the Altai Mountains. Nature 505, 43–49.

Regert, M., Bland, H.A., Dudd, S.N., Bergen, P.F.V., Evershed, R.P., 1998. Free and bound fatty acid oxidation products in archaeological ceramic vessels. Proc. Roy. Soc. Lond. B 265, 2027–2032.

Rots, V., Hayes, E., Cnuts, D., Lepers, C., Fullagar, R., 2016. Making sense of residues on flaked stone artefacts: learning from blind tests. PLoS One 11, e0150437.

Slon, V., Hopfe, C., Weiß, C.L., Mafessoni, F., de la Rasilla, M., Lalueza-Fox, C., Rosas, A., Soressi, M., Knul, M.V., Miller, R., Stewart, J.R., Derevianko, A.P., Jacobs, Z., Li, B., Roberts, R.G., Shunkov, M.V., de Lumley, H., Perrenoud, C., Gušić, I., Kućan, Z., Rudan, P., Aximu-Petri, A., Essel, E., Nagel, S., Nickel, B., Schmidt, A., Prüfer, K., Kelso, J., Burbano, H.A., Pääbo, S., Meyer, M., 2017.

584 Neandertal and Denisovan DNA from Pleistocene sediments. Science 356, 605–608.
585
586 Vahur, S., Kriiska, A., Leito, I., 2011. Investigation of the adhesive residue on the flint
587 insert and the adhesive lump found from Pulli Early Mesolithic settlement site
588 (Estonia) by micro-ATR-FT-IR spectroscopy. Est. J. Archaeol. 15, 3–17.
589
590 Vasiliev, S.K., Shunkov, M.V., Tsybankov, A.A., 2008. Faunal remains of large
591 mammals from Pleistocene deposits in the East Gallery of Denisova Cave. In
592 Problems of Archaeology, Ethnography and Anthropology of Siberia and
593 Neighbouring Territories 14, 26–31 (in Russian). Institute of Archaeology and
594 Ethnography, Siberian Branch, Russian Academy of Sciences Press, Novosibirsk.
595
596 Vasiliev, S.K., Shunkov, M.V., Tsybankov, A.A., 2010. Bone remains of large
597 mammals from Pleistocene deposits in the East Gallery of Denisova Cave (based on
598 materials obtained in 2009–2010). In Problems of Archaeology, Ethnography and
599 Anthropology of Siberia and Neighbouring Territories 16, 28–32 (in Russian). Institute
600 of Archaeology and Ethnography, Siberian Branch, Russian Academy of Sciences
601 Press, Novosibirsk.
602
603 Vasiliev, S.K., Shunkov, M.V., Kozlikin, M.B., 2013. Preliminary results on the study
604 of megafaunal remains from Pleistocene deposits in the East Gallery of Denisova
605 Cave. In Problems of Archaeology, Ethnography and Anthropology of Siberia and
606 Neighbouring Territories 19, 32–38 (in Russian). Institute of Archaeology and
607 Ethnography, Siberian Branch, Russian Academy of Sciences Press, Novosibirsk.
608
609 Vasiliev, S.K., Shunkov, M.V., Kozlikin, M.B., 2017. Megafaunal remains from the
610 Eastern Chamber of Denisova Cave and problems of reconstructing the Pleistocene
611 environments in the northwestern Altai. In Problems of Archaeology, Ethnography
612 and Anthropology of Siberia and Neighbouring Territories 23, 60–64 (in Russian).
613 Institute of Archaeology and Ethnography, Siberian Branch, Russian Academy of
614 Sciences Press, Novosibirsk.
615
616 Wadley, L., Lombard, M., 2007. Small things in perspective: the contribution of our
617 blind tests to micro-residue studies on archaeological stone tools. J. Archaeol. Sci.
618 34, 1001–1010.

FIGURE CAPTIONS

Figure 1. Images of individual saturated fatty acid micro-residues detected on artefacts DC2 and DC12 (A–E) and a typical Raman spectrum (F).

Figure 2. Example images of saturated fatty acid smeared areas on DC2, dorsal side (A), DC2, ventral side (B), DC12, dorsal side (C) and DC12, ventral side (D). Double-headed white arrows show visible striation directions.

Figure 3. Raman spectral image of smeared saturated fatty acid on the proximal left edge of artefact DC2, using the integrated area of the most intense Raman bands (C-H stretching).

Figure 4. Distribution patterns of fatty acid micro-residues and polished areas on artefacts DC2 (flake), DC4 (flake), DC12 (flake) and DC13 (retouched flake). In each image, the proximal end is up.

Figure 5. Individual mixed SFA/UFA micro-residues on artefact DC4 (A) and (B), smeared mixed SFA/UFA micro-residue on DC4 (C), association of individual mixed SFA/UFA micro-residues around a central smeared mixed SFA/UFA micro-residue (D). Double-headed white arrows show visible striation directions. Typical Raman spectrum for a mixed SFA/UFA micro-residue (E).

Figure 6. (A) Low wavenumber (1100–1700 cm^{-1}) and (B) high wavenumber (2700–3100 cm^{-1}) spectral ranges for saturated fatty acids on DC2 and DC12 (thin lines labelled ‘a’) and for mixed SFA/UFA micro-residues on DC4 and DC13 (thick lines labelled ‘b’). The unsaturation spectral markers are highlighted.

Figure 7. (A) Low wavenumber (800–1750 cm^{-1}) and (B) high wavenumber (2600–3100 cm^{-1}) spectral ranges for SFA/UFA micro-residue Raman spectra on Denisova Cave artefact DC4 (spectrum ‘a’), experimental tool D9 used to cut nettle (spectrum ‘b’), and experimental tool D3 used to scrape deer skin (spectrum ‘c’).

Table 1. Summary of analytical steps

Step	Description
1. Catalogue of unwashed artefacts	Each artefact was photographed and examined under low magnification to determine artefact class (e.g., core, flake) and to document potential traces of use.
1a. Optical microscopy of microwear and residues on selected tools	Five artefacts (DC2, DC12, DC22, DC42 and DC52) were examined under high magnification and sampled for residues with distilled water.
2. Raman microscopy of residues on artefacts prior to cleaning	Unwashed artefacts with sediment attached were examined with the Raman microscope.
3. Ultrasonication of artefacts	Artefacts were ultrasonicated for 10 s to remove loosely adhering sediment, and then air-dried. The sediments were recovered and dried in an oven for 12 hours at 70°C.
4. Raman microscopy of artefact residues and sediments	Clean artefacts were re-examined with the Raman microscope by systematically scanning all artefact edges with a 50× objective on both sides (dorsal and ventral), within a strip approximately 200 µm from the edge. The remaining artefact surface was scanned with a 20× objective to confirm the extent and depth of micro-residue concentrations. The sediment removed from the artefacts and oven-dried was also analysed with the Raman microscope.
5. Optical microscopy and mapping of use-polish	Artefacts were examined under high magnification, vertical incident light to map the distribution of use-polish along any utilised edges. Use-polish was described as one of three qualitative forms: (1) continuous polish present in narrow bands along an edge or in continuous alignments away from the edge; (2) discontinuous polish along part of an edge and scattered alignments or zones of polish on surfaces away from the edge; and (3) developed polish extending both along the edge and away from it.
6. Optical microscopy of usewear and residues	Clean artefacts were examined under high magnification stereo and vertical incident light microscopes to characterise use-polish and other traces of use to identify the worked materials and modes of use (e.g., cutting, sawing, scraping).

Table

Table 2. Summary of experimental micro-residue analysis

Artefact	Material worked	Aging time	Use	Residues analysed	Frequency
			SET 1		
X290	Fresh possum skin (*Trichosurus vulpecula*)	30 years	Scraping	**Smeared SFA** **Individual SFA** Protein fibre Protein Starch grain	Very Common Very Common Common Common Rare
X284	Dry cow bone (*Bos taurus*)	30 years	Sawing	Bone + collagen Smeared bone **Smeared SFA** + bone **Smeared SFA**	Very common Very common Common Uncommon
X288	Meat (*Bos taurus*)	30 years	Cutting	Collagen fibre Smeared protein SFA fibre **Individual SFA**	Very common Very common Uncommon Uncommon
X309	Fresh cow bone (*Bos taurus*)	30 years	Scraping	Bone + collagen Collagen fibre (protein) Lipids Plant fibre	Very common Very common Uncommon Rare
SET 2					
D1	Fresh fallow deer bone (*Dama dama*)	3 months	Cleaning Extracting marrow Scraping	Smeared bone + collagen Bone + collagen **Smeared mixed SFA/UFA**	Very common Very common Uncommon
D2	Fresh fallow deer jaw bone (*Dama dama*)	3 months	Sawing	Bone + collagen Smeared bone + collagen **Smeared mixed SFA/UFA** Protein	Very common Very common Uncommon Rare
D3	Fresh fallow deer skin (*Dama dama*)	3 months	Scraping	**Smeared mixed SFA/UFA** **Individual mixed SFA/UFA** Collagen fibre (protein) Protein	Very Common Very Common Uncommon Uncommon
D4	Fern (*Athyrium filix-femina*)	2 weeks	Cutting	Plant fibre Chlorophyll Smeared chlorophyll	Common Common Common
D5	Rowan (*Sorbus aucuparia*)	2 weeks	Cutting Scraping	Wood fibre Smeared wood fibre Oxalate **Individual SFA**	Common Common Rare Rare
D8	Siberian pine (*Pinus sibirica*)	1 month	Cutting Scraping	Smeared wood Wood fibre Plant fibre Smeared resin	Common Common Uncommon Uncommon
D9	Nettle (*Urtica dioica*)	9 months	Cutting	Plant fibre **Smeared mixed SFA/UFA** **Individual mixed SFA/UFA**	Common Common Common
D10	Birch bark (*Betula pendula*)	1 month	Cutting	Smeared wood Wood fibre Fluorescent plant fibre	Common Common Uncommon
D11	Tussock grass (*Poa labillardierei*)	1 day	Cutting	Plant fibre Smeared plant fibre **Smeared mixed SFA/UFA** **Individual mixed SFA/UFA** Starch grain Oxalate	Common Common Uncommon Uncommon Uncommon Uncommon

SFA: saturated fatty acids
UFA: unsaturated fatty acids
SFA/UFA: saturated fatty acid /unsaturated fatty acid mix

Table 3. Comparison of proposed prehistoric use of the artefacts based on Raman spectroscopy and optical microscopy results

Specimen details			Raman spectroscopy			Optical microscopy	
Artefact	**Layer**	**Artefact class**	**Significant archaeological residue**	**Proposed origin of residue**	**Task determined according to polish distribution**	**Material worked**	**Mode of use**
DC1	11.4	Retouched flake	ND	NA	Uncertain	Animal	Scraping, cutting
DC2	11.4	Flake	**SFA**	Animal fat	Cutting	Animal	Cutting
DC4	11.4	Flake	**Mixed SFA/UFA**	Animal fat	Scraping, cutting	Uncertain	Uncertain
DC12	11.4	Flake	**SFA**	Animal fat	Scraping	Uncertain	Scraping
DC13	11.4	Retouched flake	**Mixed SFA/UFA**	Animal fat	Scraping	Animal skin	Scraping
DC39	11.4	Flake	**Mixed SFA/UFA**	Animal fat	Cutting	Flesh and bone	Butchering
DC42	12.2	Retouched flake	ND	NA	Not used	None	Not used
DC52	12.2	NDA	ND	NA	Not used	None	Not used
DC43	12.3	Kombewa flake	ND	NA	Uncertain	Flesh and bone	Scraping
DC45	12.3	Retouched flake	ND	NA	Scraping	Flesh and bone	Scraping, cutting
DC5	13	Retouched flake	ND	NA	Uncertain	Flesh and bone	Scraping
DC14	13	Flaked piece	ND	NA	Not used	None	Not used
DC26	13	Split flake	**SFA'**	Animal fat	Scraping, cutting	Uncertain	Unknown
DC27	13	Retouched flake	**SFA'**	Animal fat	Scraping, cutting	Flesh and bone	Scraping, cutting, butchering
DC30	13	Flake	ND	NA	Not used	Uncertain	Scraping
DC11	15	Retouched flake	**Mixed SFA/UFA**	Animal fat	Scraping, cutting	Flesh and bone	Scraping, cutting, sawing
DC22	15	Flaked piece	ND	NA	Not used	None	Not used
DC23	15	Flaked piece	ND	NA	Not used	None	Not used

NA: not applicable
ND: not detected
SFA: saturated fatty acid
SFA': saturated fatty acid with different composition
SFA/UFA: saturated fatty acid /unsaturated fatty acid mix

Table

Table 4. Summary of Raman results for artefacts DC2, DC12, DC4 and DC13

Artefact	Organic and mineral residues on artefact surface	Minerals and residues in inner and outer sediment	Minerals and residues in washed sediment	Mineral background
DC2	Apatite (very common) Smeared SFA (common) Individual SFA (common) Protein (uncommon) Starch grain (uncommon) Plant fibre (uncommon) Cellulose fibre* (rare) Plastic box* (rare)	Apatite (very common) Feldspar (common) Quartz (common)	Apatite (very common) Feldspar (common) Quartz (common) Mica (uncommon) Epidote (uncommon)	Mica Feldspar Quartz
DC12	Apatite (very common) Smeared SFA (common) Individual SFA (uncommon) Protein (uncommon) Plant fibre* (uncommon) Starch grain (uncommon) Unknown small fibre* (rare) Plant fibre dyed* (rare)	Apatite (very common) Calcite (common) Feldspar (common) Quartz (common)	Apatite (very common) Calcite (common) Feldspar (common) Quartz (common) Epidote (uncommon)	Mica Epidote Feldspar Quartz
DC4	Apatite (very common) Individual mixed SFA/UFA (common) Smeared mixed SFA/UFA (common) Protein (uncommon) Geological apatite (uncommon) Starch grain (rare) Calcite (uncommon)	Apatite (very common) Calcite (common) Feldspar (common) Quartz (common) Plant fibre (rare)	Apatite (very common) Feldspar (common) Quartz (common) Mica (uncommon)	Feldspar Hornblende Quartz
DC13	Apatite (very common) Smeared mixed SFA/UFA (uncommon) Individual mixed SFA/UFA (uncommon) Protein (rare) FA fibre (rare)	Apatite (very common) Feldspar (common) Quartz (common) Gypsum (uncommon)	Apatite (very common) Feldspar (common) Quartz (common) Calcite (uncommon)	Feldspar Quartz

Relative occurrence:

Very common: micro-residues are widespread and found very easily
Common: micro-residues detected easily, but only in limited areas or with specific distributions
Uncommon: micro-residues not easy to detect and occur in fewer numbers in spatially constrained areas
Rare: micro-residues found very infrequently on the artefact and in the sediment
NC: not counted
Asterisk (*): modern contaminants

Figure

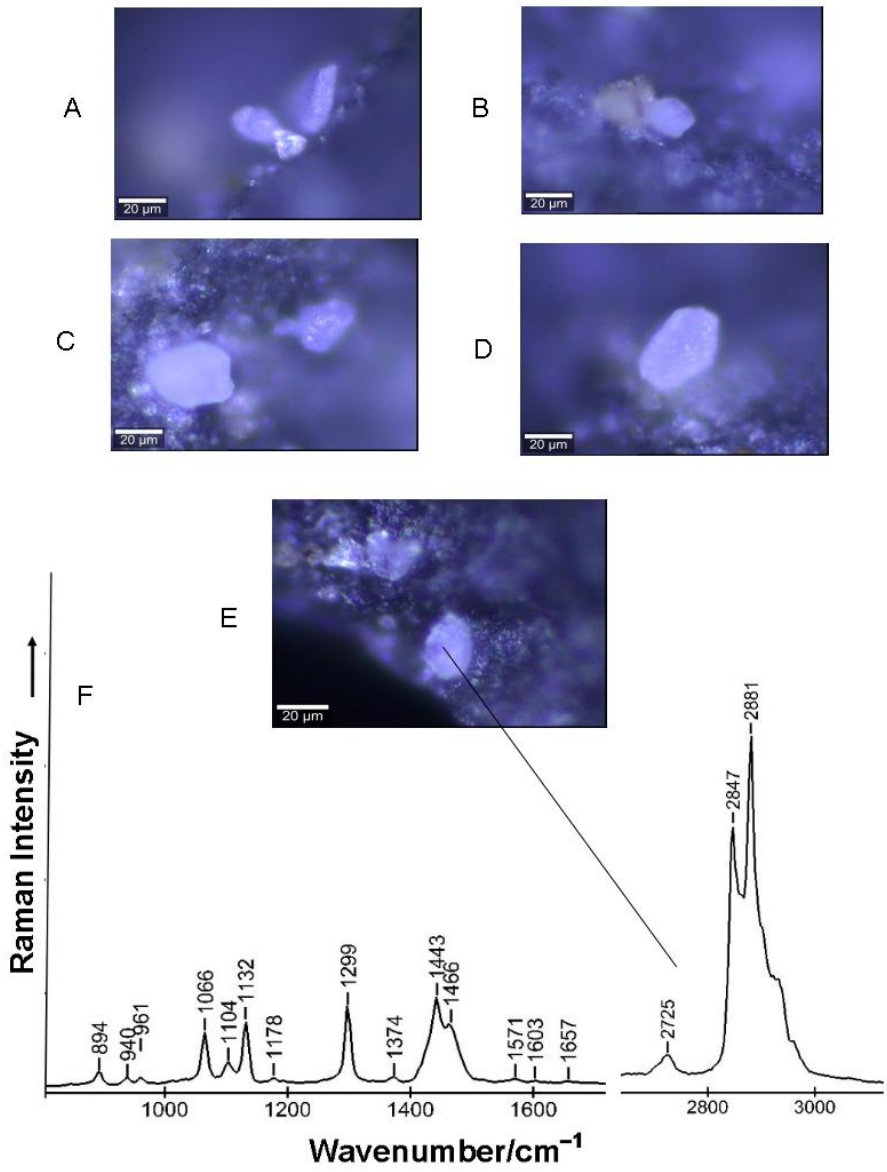
A
B
C
D
E
F
20 μm
Raman Intensity
894
940
961
1066
1104
1132
1178
1299
1374
1443
1466
1571
1603
1657
2725
2847
2881
1000
1200
1400
1600
2800
3000
Wavenumber/cm⁻¹

Figure

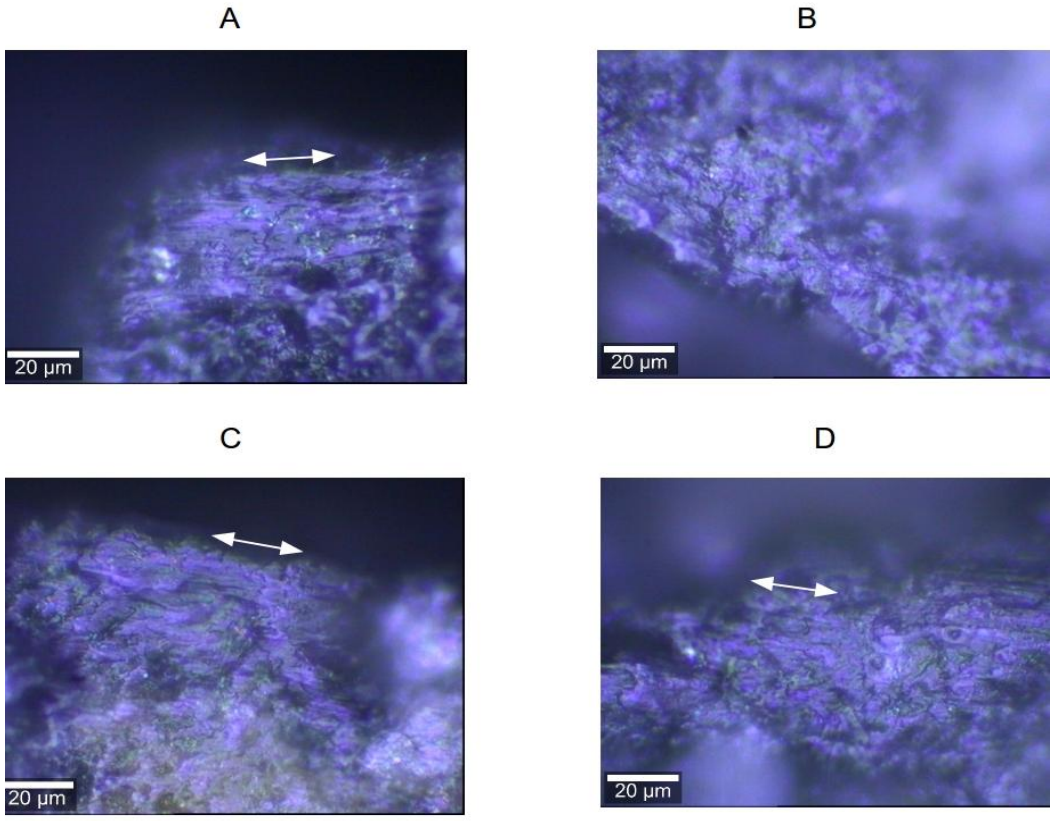

Figure

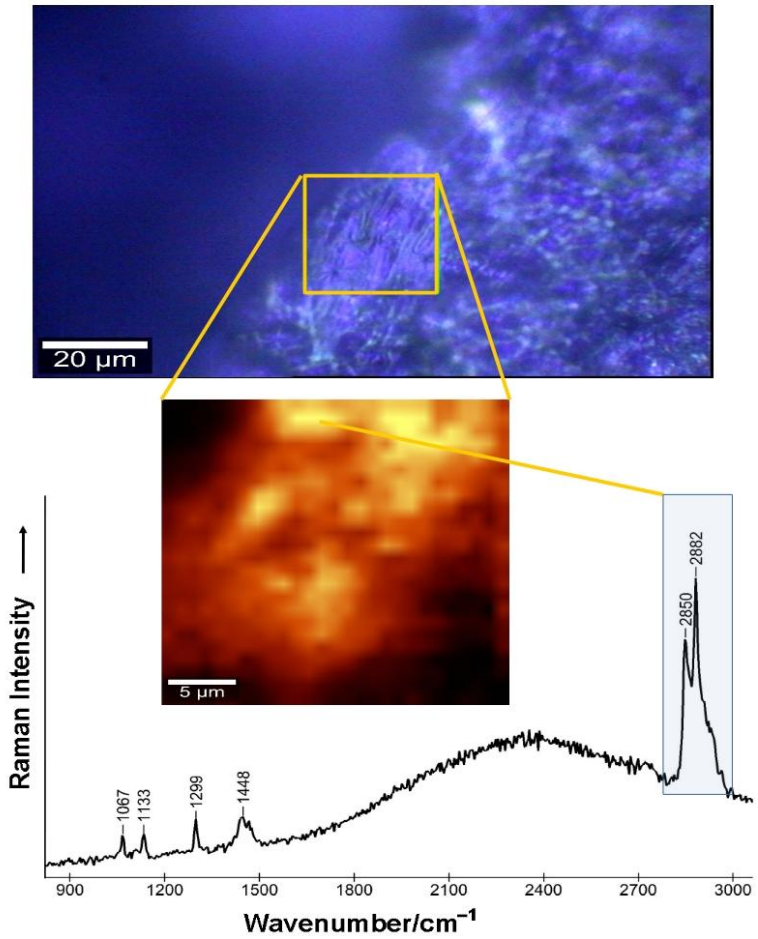
20 µm
5 µm
Raman Intensity
1067
1133
1299
1448
2850
2882
900
1200
1500
1800
2100
2400
2700
3000
Wavenumber/cm⁻¹

Figure

Click here to download high resolution image

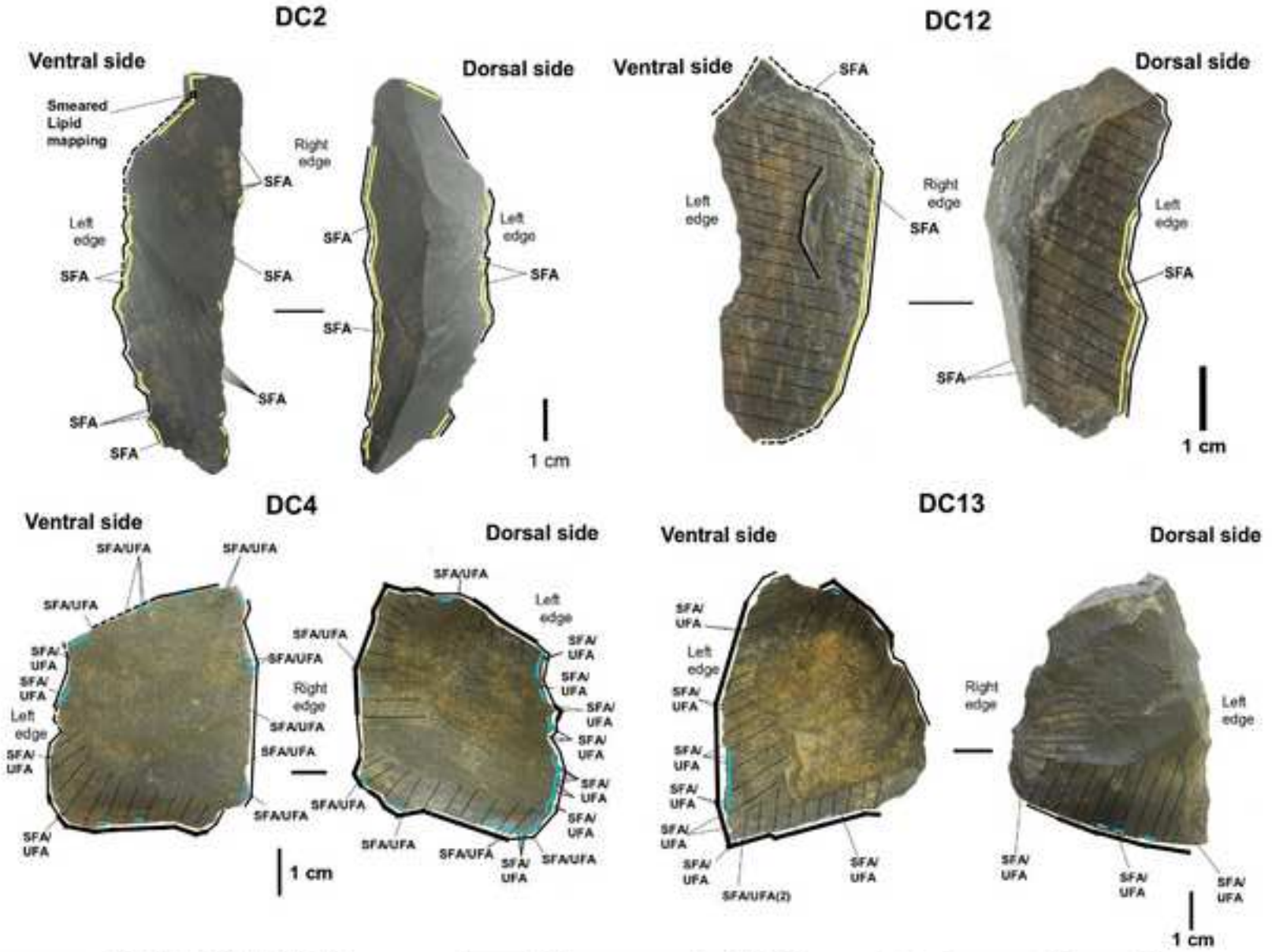

Figure

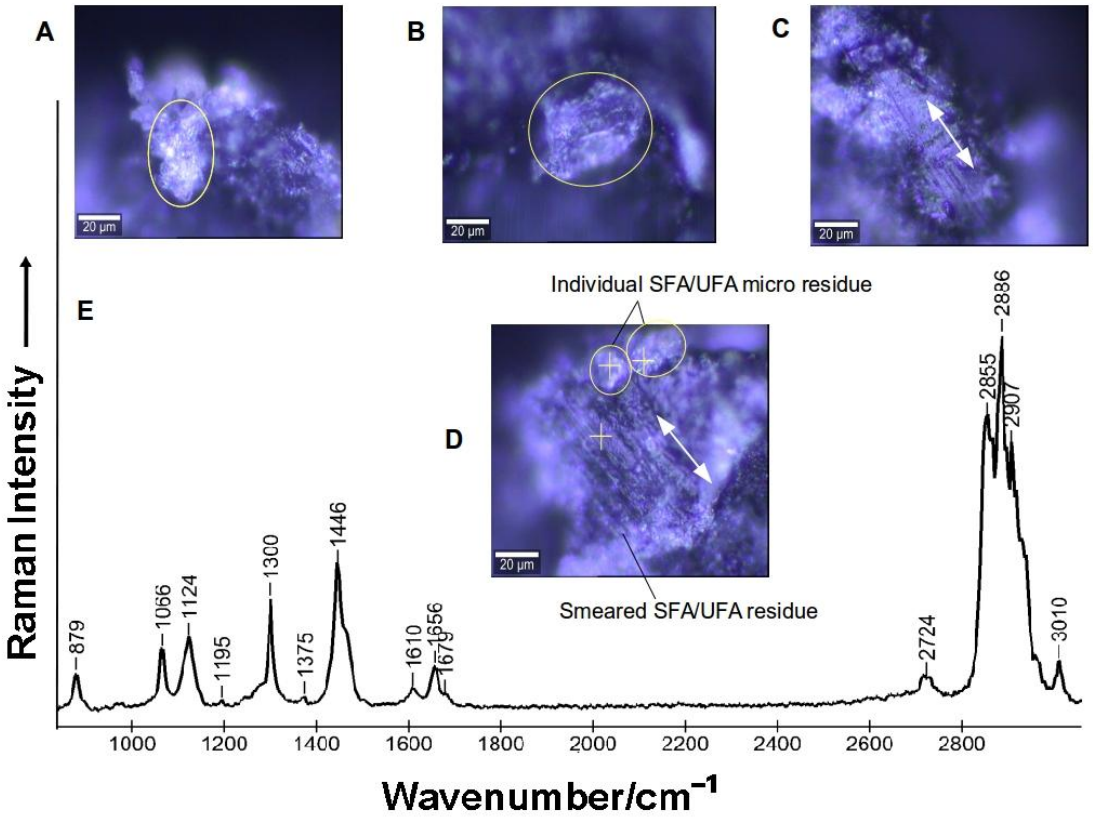
A
B
C
D
E
20 µm
Individual SFA/UFA micro residue
Smeared SFA/UFA residue
Raman Intensity
Wavenumber/cm^{-1}
879
1066
1124
1195
1300
1375
1446
1610
1656
1679
2724
2855
2886
2907
3010
1000
1200
1400
1600
1800
2000
2200
2400
2600
2800

Figure

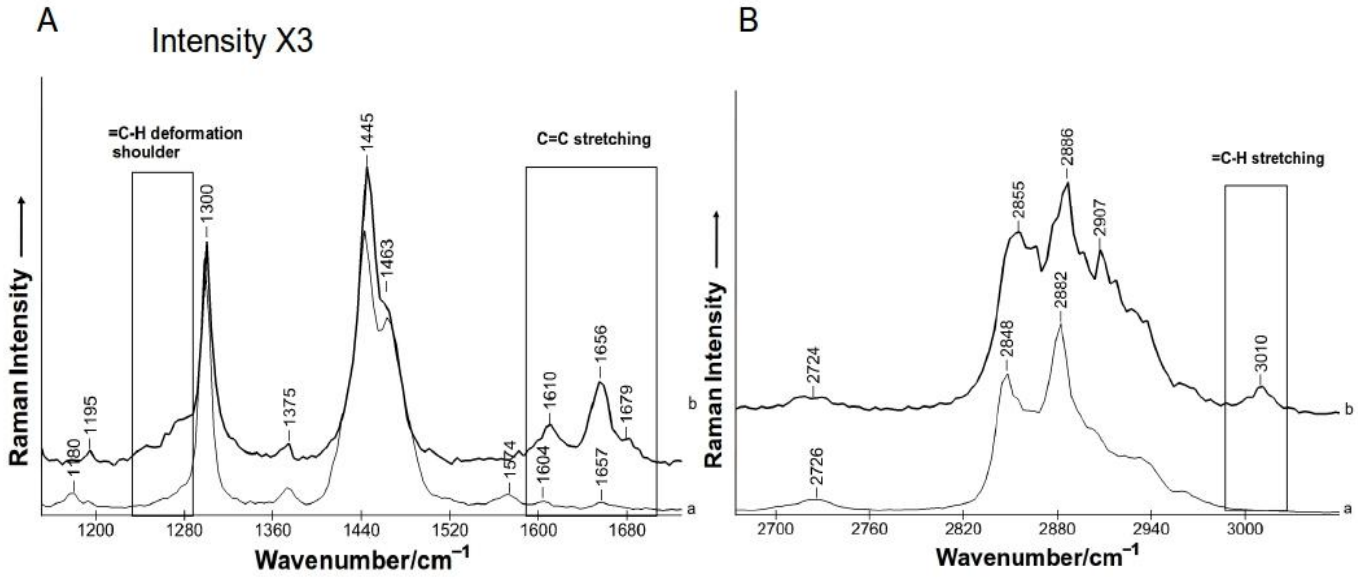
A
Intensity X3
=C-H deformation shoulder
C=C stretching
1300
1445
1463
1195
1180
1375
1610
1656
1679
1574
1604
1657
Raman Intensity
b
a
1200
1280
1360
1440
1520
1600
1680
Wavenumber/cm−1
B
2886
2855
2907
2882
2848
2724
2726
3010
=C-H stretching
Raman Intensity
b
a
2700
2760
2820
2880
2940
3000
Wavenumber/cm−1

Figure

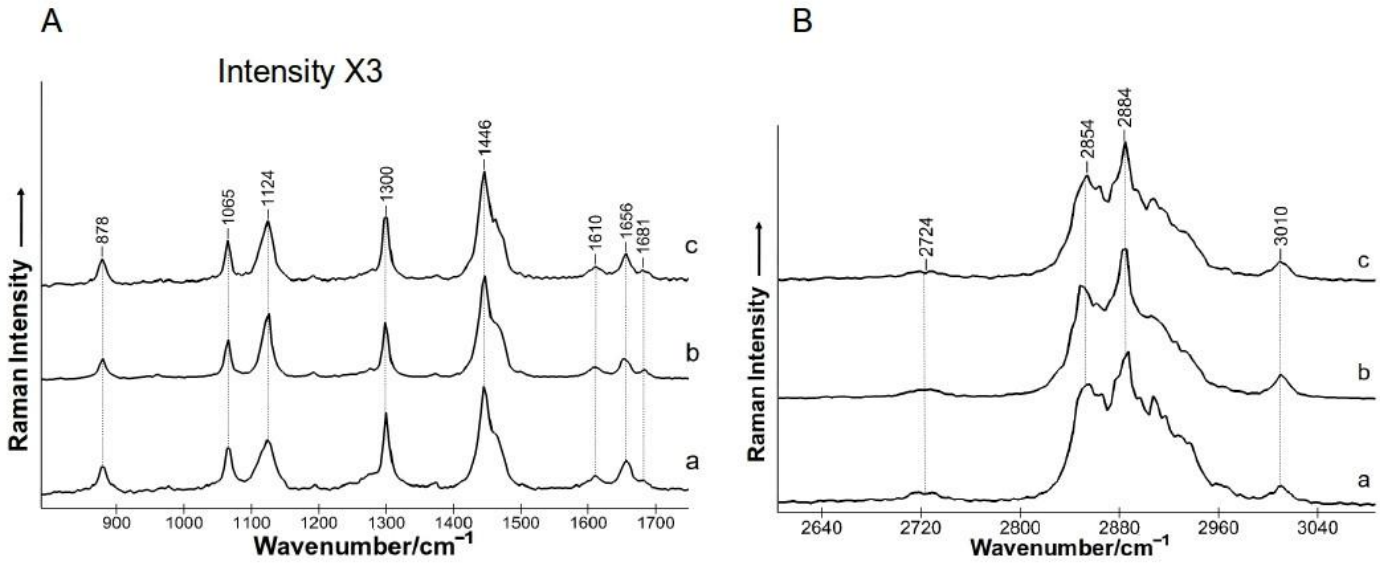
A
Intensity X3
Raman Intensity
878
1065
1124
1300
1446
1610
1656
1681
c
b
a
900
1000
1100
1200
1300
1400
1500
1600
1700
Wavenumber/cm⁻¹
B
Raman Intensity
2724
2854
2884
3010
c
b
a
2640
2720
2800
2880
2960
3040
Wavenumber/cm⁻¹